NASA Technical Memorandum 83595

Factors Which Influence Directional Coarsening of γ' During Creep in Nickel-Base Superalloy

Rebecca A. MacKay
Lewis Research Center
Cleveland, Ohio

and

Lynn J. Ebert
Case Western Reserve University
Cleveland, Ohio

Prepared for the
Fifth International Symposium on Superalloys
sponsored by the American Institute of Mining,
Metallurgical and Petroleum Engineers
Seven Springs, Pennsylvania, October 7-11, 1984

NASA

FACTORS WHICH INFLUENCE DIRECTIONAL COARSENING OF γ' DURING CREEP IN NICKEL-BASE SUPERALLOY SINGLE CRYSTALS

Rebecca A. MacKay
National Aeronautics and Space Administration
Lewis Research Center
Cleveland, Ohio 44135 U.S.A.

and

Lynn J. Ebert
Case Western Reserve University
Department of Metallurgy and Materials Science
Cleveland, Ohio 44106 U.S.A.

Summary

Changes in the morphology of the γ' precipitate were examined as a function of time during creep at 982°C in [001] oriented single crystals of a Ni-Al-Mo-Ta superalloy. In this alloy, which has a large negative misfit of -0.80 pct., the γ' particles link together during creep to form platelets, or rafts, which are aligned with their broad faces perpendicular to the applied tensile axis. The effects of initial microstructure and alloy composition on raft development and creep properties were investigated specifically in this study. The results show that directional coarsening of γ' begins during primary creep and continues to develop well after the onset of second-stage creep. The thickness of the rafts, however, remains constant up through the onset of tertiary creep; this is a clear indication of the stability of the finely-spaced γ/γ' lamellar structure. Furthermore, the thickness of the rafts which formed was equal to the initial γ' size which was present prior to testing. It was found that the single crystals with the finest γ' size exhibited the longest creep lives, because the resultant rafted structure had a larger number of γ/γ' interfaces per unit volume of material, which provided additional barriers to dislocation motion. It was also shown that reducing the Mo content by only 0.73 wt. pct. increased the creep life by a factor of three, because the precipitation of a third phase was eliminated.

Introduction

Changes in the morphology of the γ' precipitate have been observed in nickel-base superalloys which were subjected to external stresses at elevated temperatures (1-3). Coarsening of the γ' particles reduced the creep resistance in these polycrystalline materials, because the overaged microstructure allowed deformation to occur by particle by-passing (1,3). However, recent studies (4,5) on nickel-base superalloy single crystals with a large negative mismatch in lattice parameter, where $a(\gamma) > a(\gamma')$, have demonstrated that directional coarsening of γ' significantly improved high temperature creep properties in the [001] orientation. The fine and continuous γ' platelets, or rafts, which formed were believed to improve the creep resistance of this material by providing effective barriers to dislocation climb around γ'. The suppression of this creep deformation mechanism would force the dislocations to shear the γ' rafts, which, in turn, would be retarded in this microstructure by the dense networks of misfit dislocations formed at the γ/γ' interfaces.

The purpose of the present study is to examine the kinetics of the formation and subsequent development of directional coarsening of γ' in nickel-base superalloy single crystals during creep at 982°C and 234 MPa. The influences of the initial microstructure and slight compositional variations on the raft development and creep properties were investigated specifically.

Dr. C. S. Kortovich of TRW, Inc. provided the single crystal material. Dr. D. D. Pearson of the United Technologies Research Center participated in many valuable discussions.

Materials and Experimental Procedures

Single crystals with two slightly different compositions were cast in the [001] direction; these compositions are given in Table I. The 1.25 cm diameter single crystal bars were heat treated above the γ' solvus in an argon atmosphere at 1313°C for 100 hours to produce chemical homogeneity. The bars then were forced air quenched to ambient temperature. Specimens with a 0.48 cm gage diameter and a 1.90 cm gage length were machined from the heat treated bars.

Table I. Compositions of Single Crystal Alloys (wt. pct.)

	Elements			
Alloy Designation	Al	Mo	Ta	Ni
Alloy 1	5.80	14.63	6.24	balance
Alloy 2	6.05	13.90	5.85	balance

Three different γ' sizes were produced in the single crystals prior to creep testing by: (a) forced air quenching from the homogenization temperature; (b) forced air quenching plus aging at 982°C for 115 hours; and (c) oil quenching from the homogenization temperature. The specimens in (c) actually were re-solutionized above the γ' solvus in the fully homogenized, machined bar form and then were quenched into oil. Thus, these latter specimens were given a more severe quench, not only because of the quenching medium, but because of the smaller section size as well.

Single crystal specimens having orientations within 10° of the [001] then were creep tested in tension under constant load at 982 ± 2°C and 234 MPa. Upon completion of testing, specimens were sectioned parallel to

the applied stress axis and examined by means of scanning electron microscopy (SEM). A line intercept technique was used on the SEM photos of tested specimens in order to obtain measurements of γ' raft length, γ' raft thickness, and interlamellar spacing.

Results and Discussion

γ' Shape Changes in Baseline Material

The forced air quenched single crystals had a conventional superalloy microstructure, prior to testing, which consisted of γ' cubes in a γ matrix. An example of this microstructure is shown in Figure 1a. Misfit dislocations which formed during the quench from the homogenization temperature may be seen at the γ/γ' interfaces. This microstructure was considered to be the baseline condition. The mismatch in lattice parameter in this alloy was measured to be -0.80 percent (6).

(a) (b) (c)

Figure 1. The γ' precipitate and dislocation structure is shown in single crystals after heat treating and (a) forced air quenching, (b) aging at 982°C for 115 hours, and (c) oil quenching.

A typical creep curve at 982°C and 234 MPa is depicted in Figure 2 for the air quenched single crystals. The corresponding microstructures of the specimens which were interrrupted at various times during creep also are shown in Figure 2. These micrographs illustrate the development of directional coarsening of γ' from a cuboidal to a plate-like morphology, which is oriented perpendicular to the applied stress axis. The acicular phase present in these micrographs is the NiMo δ phase which precipitates during creep testing because of a supersaturation of molybdenum in Alloy 1. As shown in Figure 2, the γ' particles started to link together early during primary creep. The γ' rafts continued to develop well into steady-state creep, as is indicated by their increased lateral extension. After about 50 hours of creep testing, the γ' rafts extended completely across the micrograph from one side to the other and were about as fully developed as possible. The raft thickness appeared to remain constant throughout most of the creep test; however in the failed condition, the lamellae were considerably coarser.

In order to quantify this changing morphology during creep, the mean raft dimensions were measured and were plotted as a function of time in Figure 3. Each data point in this figure represents between 150 and 250 measured γ' particles or rafts in each specimen. The times to the onset of steady-state creep, t_s, and to the onset of tertiary creep, t_t, also are indicated in the figure for comparison to the creep curve in Figure 2.

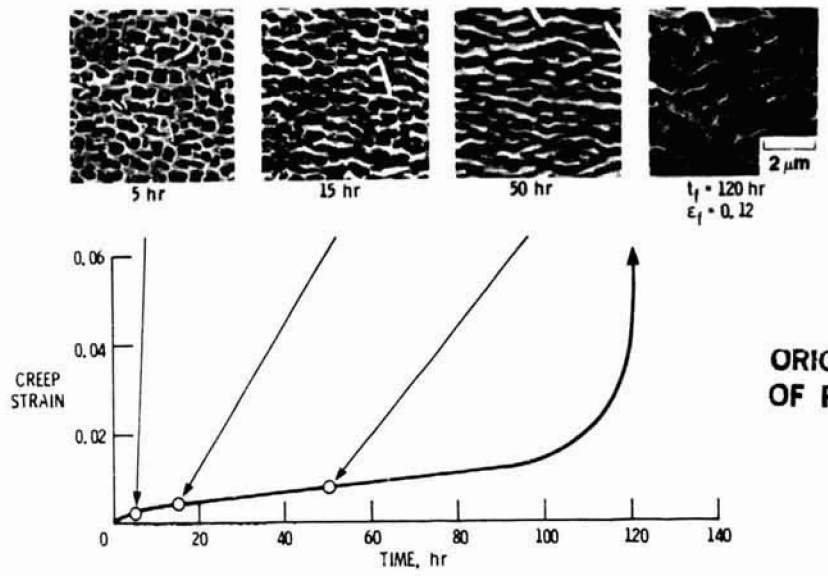

Figure 2. A typical creep curve is illustrated at 982°C and 234 MPa with corresponding micrographs which show the development of directional coarsening of γ' during creep.

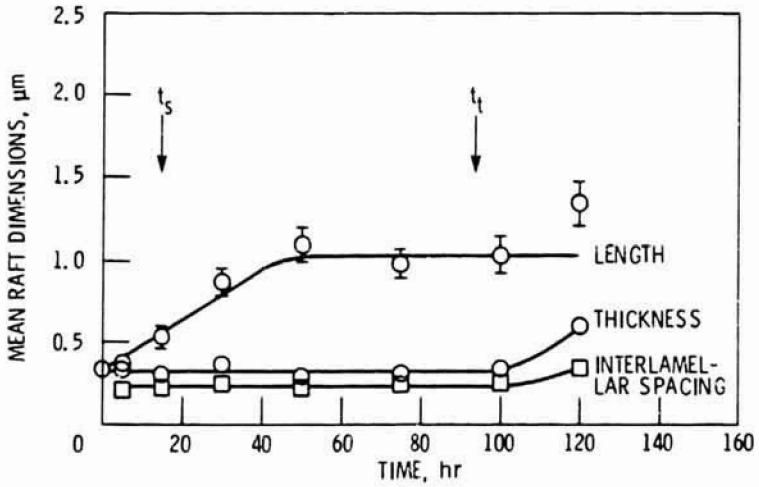

Figure 3. The mean dimensions of the γ' rafts are plotted as a function of time during creep at 982°C and 234 MPa.

As shown in Figure 3, the mean raft length increases linearly with time from zero up to almost 50 hours of creep testing. At this point, the crystal is well into steady-state creep, and the values of the raft lengths reach a plateau and remain constant thereafter. This plateau appears to correspond to the point when the microstructure consists of continuous, interconnected γ' lamellae. However, an average intercept length of only 1.0 μm was measured throughout the plateau region, due to irregularities in the lamellae. Since the γ' particles continued to directionally coarsen during secondary creep, it appears that the formation of the γ' rafts is not related directly to the onset of second-stage creep. Apparently, sufficient strain hardening for the transition into steady-state creep is attained prior to the onset of the plateau in mean raft length. The mean raft length in the failed specimen was measured as having a slightly higher value than that of the plateau. However, this observation appears to be at least partially the result of the considerably thickened plates in the failed condition, which would allow a longer intercept length to be mea-

sured. As a result, the line for the plateau in Figure 3 was not drawn to connect the data point at 120 hours.

In contrast to the raft length, the mean raft thickness remained constant, at 0.33 μm, from the start of the test up through the onset of tertiary creep, as is illustrated in Figure 3. However, single crystals in the failed condition have undergone a substantial increase in the total amount of strain during tertiary creep, and the rafts in the failed condition have coarsened considerably. As may be noted in Figure 3, this increase in thickness was rather abrupt, because the specimen interrupted at 100 hours, which was after the onset of tertiary creep, showed no increase in raft thickness. The interlamellar spacing, or thickness of the γ phase, also is plotted as a function of time in Figure 3, and these data display the same behavior as the raft thickness data. The behavior of the γ' raft thickness and interlamellar spacing during creep is a clear indication of the stability of the finely-spaced rafted structure. This is also an important difference from the observations in other alloys in which agglomeration of γ' into stringer-like configurations proceeded slowly during creep (7), and the interparticle spacing increased as the γ' coarsened under stress (1,3). However, the directional coarsening behavior exhibited by the present Ni-Al-Mo-Ta alloy appears similar to that observed in a more conventional single crystal superalloy, NASAIR 100 (8).

Effect of Initial Microstructure

Significantly different microstructures were produced in the single crystals of Alloy 1 prior to creep testing. The baseline, air quenched microstructure in Figure 1a has been described previously. The microstructure after 115 hours of aging at 982°C is shown in Figure 1b; it consists of γ' particles which had coarsened from the baseline size of 0.33 μm to a size of 0.44 μm. In addition, three-dimensional hexagonal arrays of misfit dislocations were present in the γ/γ' interfaces in the aged structure. Oil quenching refined the γ' size to 0.15 μm, and reduced the interparticle spacing, as is indicated in Figure 1c. In addition, the γ' cuboids appeared to be more aligned along cube directions; and misfit dislocations were absent.

These three initial microstructures had a significant effect on the subsequent creep properties at 982°C and 234 MPa, as shown by the creep curves in Figure 4. The aged specimen had a creep life which was equal to about half of the life of the baseline specimen. Oil quenching increased

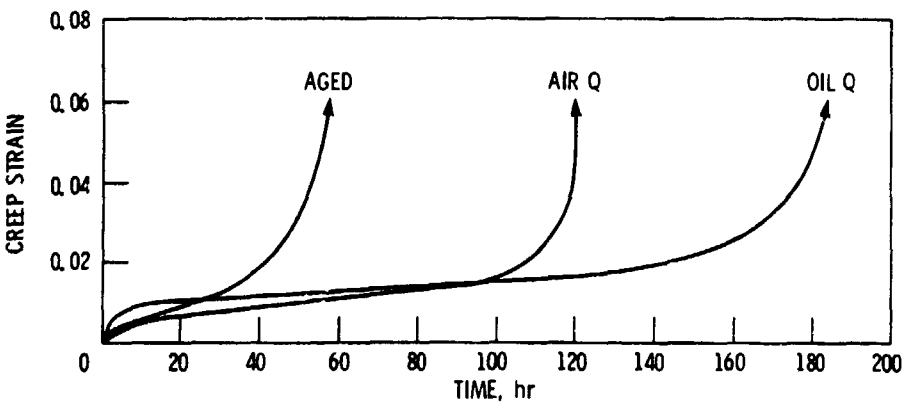

Figure 4. Creep curves at 982°C and 234 MPa are illustrated for single crystals in the aged, air quenched, and oil quenched conditions.

the life from the baseline of 120 to 189 hours, and reduced the steady-state creep rate by a factor of two. These microstructure-property relations for the present alloy are analogous to those in other studies which showed that coarse γ', caused by overaging, degraded the creep properties in polycrystalline materials (3,9). However, the increase in creep life achieved as a result of a more rapid quench from the homogenization temperature was not anticipated.

The mean raft dimensions for the aged and oil quenched specimens have been plotted as a function of time during creep in Figures 5a and b, respectively. The values of t_s and t_t are indicated in these figures for comparison to the creep curve of each respective specimen. Superimposed on these data are the raft dimensions for the baseline single crystals from Figure 3. The kinetics for rafting were estimated by the positive slope of the mean raft length versus time data displayed in Figures 5a and b. As shown in Figure 5a, the raft length versus time data for the aged specimens were offset but parallel to that for the baseline material. So although the γ' had coarsened to 0.44 μm and had extensive misfit dislocation networks, the kinetics for rafting during creep in the aged single crystals

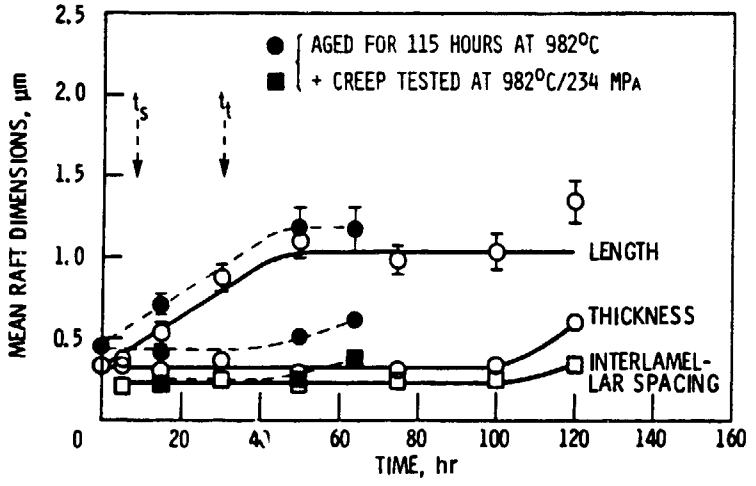

(a)

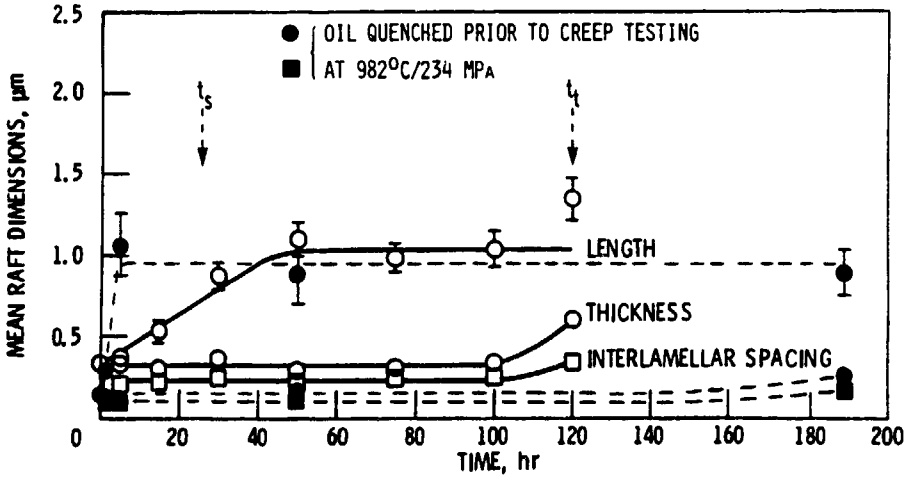

(b)

Figure 5. The mean raft dimensions are plotted as a function of time during creep for the (a) aged and (b) oil quenched crystals. The open symbols represent the raft dimensions for the air quenched crystals, shown previously in Figure 3.

were equal to that for the baseline material. The plateau, which occurred when the rafts were fully developed, began in the aged crystals after the onset of tertiary creep. The γ' rafts were coarser in the aged specimens, because the initial γ' size was larger.

The mean raft dimensions of the oil quenched crystals are illustrated in Figure 5b. The rafting rate was at least ten times faster in this condition that in the baseline material. The plateau in mean raft length for the oil quenched specimens was attained prior to the onset of steady-state creep, and occurred after only about five hours. The thickness of the rafts remained constant at the starting γ' size of 0.15 μm, and as a result, the lamellae were considerably finer, even in the failed condition.

Thus, the initial microstructures prior to testing can drastically affect the subsequent rafting kinetics. For example, the closely-spaced γ' particles in the oil quenched single crystals may have hastened the development of the rafts, because the distance for diffusion was reduced. In addition, the rafting kinetics may be influenced by misfit dislocations present prior to testing. Since one of the driving forces for directional coarsening is the reduction in elastic strain energy (10), the presence of misfit dislocations, which consume the elastic coherency strains, can reduce the rate at which the rafts form. This may have had some effect in the aged and air quenched single crystals which contained misfit dislocations prior to testing and exhibited lower rafting rates.

The disparity in rafting rates between the different starting microstructures may contribute somewhat to the differences in creep properties. However, the air quenched and aged specimens exhibited similar rafting rates, and yet their creep lives were significantly different. The reason for such differences in properties seems to be related to the γ/γ' interfacial area per unit volume of material. For a specific γ' volume fraction, a larger number of interfaces are present with a finer γ' raft thickness, which can be produced by a refinement of the initial γ' size. Since it is believed that the misfit dislocation networks at the γ/γ' interfaces provide an effective impedance to matrix dislocation motion (4,5), then a larger number of interfaces per unit volume should reduce the creep deformation rate and improve creep properties. Figure 6 shows the microstructures of the air quenched, aged, and oil quenched single crystals after 50 hours of testing at 982^{o}C and 234 MPa. Comparison of these micrographs with the creep curves in Figure 4 shows that the properties improved substantially as the raft thickness decreased and the number of γ/γ' interfaces increased.

Figure 6. The γ/γ' lamellae are shown after 50 hours of creep testing at 982^{o}C and 234 MPa in the (a) air quenched, (b) aged, and (c) oil quenched crystals.

Third Phase Precipitation

The needle-like third phase which precipitated during creep was identified as NiMo δ. The amount of δ present was measured by phase extraction to be about 0.85 wt. pct and about 2.0 wt. pct. by quantitative metallography. The δ phase caused some undesirable microstructural features. Specifically, envelopes of γ' formed around the δ needles, and these envelopes became more prominent as the creep exposure time increased. An example of the discontinuities in the γ/γ' lamellar structure which were caused by the δ needles is shown in Figure 7. Such discontinuities could provide paths for mobile dislocations to circumvent the γ/γ' interfaces, thereby reducing the effectiveness of the lamellar structure. The microstructural changes caused by δ appeared to be more pronounced in the oil quenched material, because the thickness of the γ' envelopes which encapsulated the δ needles was much coarser than the thickness of the γ/γ' lamellae. As a result, the full potential of the rafted structure could not be attained with this composition, even with the refinement of the initial γ' size.

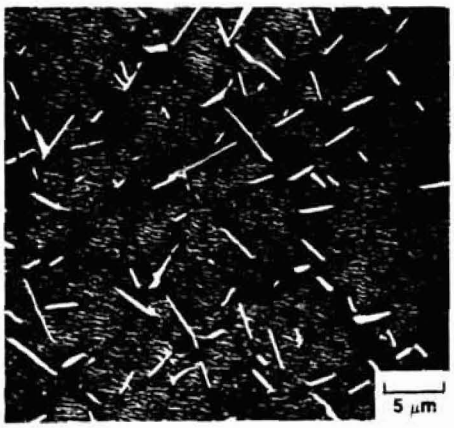

Figure 7. Discontinuities are shown in the γ/γ' lamellar structure, which were caused by δ needles with surrounding envelopes of γ', in an oil quenched crystal after 189 hours of testing at 982^{o}C and 234 MPa.

Another Ni-Al-Mo-Ta single crystal composition having a slightly lower Mo content was examined to determine the creep properties of a similar alloy which did not contain δ. As indicated in Table I, the Mo level in this second alloy was only 0.73 wt. pct. lower than that in Alloy 1. There were also small differences in the Al and Ta contents in Alloy 2 which may have changed the solubility of Mo in the matrix, although these effects appear to have been second-order with respect to that of the Mo content. As shown in Figure 8, significant improvements in creep life and steady-state creep rate were attained in the lower Mo alloy when tested under the same conditions of 982^{o}C and 234 MPa. Although the properties of the 14.6 wt. pct. Mo alloy were still superior to most conventional superalloy single crystals (6), the creep life tripled in the air quenched condition when the Mo content was reduced from 14.6 to 13.9 wt. pct. The microstructure of the failed single crystal of the lower Mo alloy showed that very little δ was present after 356 hours of creep testing at 982^{o}C. Thus, the alloy containing 13.9 wt. pct. Mo was very close to being saturated with Mo, but without being supersaturated, as was the case in the 14.6 wt. pct. Mo alloy.

The increase in creep life, which was realized when the single crystals were oil quenched to refine the γ' size, was even more dramatic in the lower Mo alloy than in Alloy 1. This is demonstrated clearly in Figure 8.

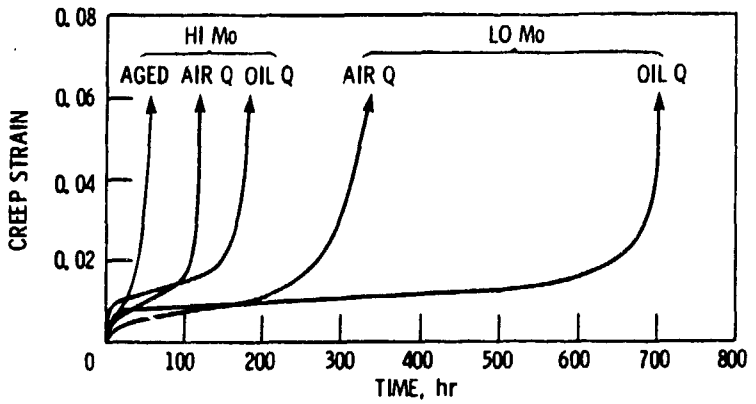

Figure 8. Creep curves at 982°C and 234 MPa are illustrated for the 14.6 and 13.9 wt. pct. Mo alloys in the aged, air quenched, and oil quenched conditions.

For example, in the 14.6 wt. pct. Mo alloy, the life increased from 120 hours to 189 hours when an oil quench was performed prior to testing; the steady-state creep rate decreased correspondingly by a factor of two. However, in the 13.9 wt. pct. alloy, the life of the single crystal increased from 356 to 705 hours when the specimen was oil quenched; the steady-state creep rate decreased by a factor of over three. Thus, making slight compositional modifications improved the creep life of the baseline, air quenched material by a factor of three. However, refining the initial γ' size from 0.33 to 0.15 μm with an oil quench from the homogenization temperature, in addition to lowering the Mo content, increased the creep life by a factor of six.

Conclusions

The γ' particles in this -0.80 pct. misfit alloy began to directionally coarsen during primary creep at 982°C and 234 MPa. The length of the γ' rafts increased linearly up to a plateau, which was reached well after the transition into second-stage creep occurred. The thickness of the rafts remained constant from the start of the creep test up through the onset of tertiary creep. The interlamellar spacing followed a similar behavior to the raft thickness data as a function of time; and this is a clear indication of the stability of this continuous and finely-spaced directionally coarsened structure.

Gamma prime sizes ranging from 0.15 to 0.44 μm were produced in different single crystal specimens prior to creep testing. The thickness of the rafts which formed was equal to the initial γ' size. The single crystals with the finest γ' size exhibited the longest creep lives, because the rafts which formed had a larger γ/γ' interfacial area per unit volume. A large number of interfaces would provide additional barriers to matrix dislocation motion, thereby improving the creep resistance of the material.

Reducing the Mo content in this alloy by only 0.73 wt. pct. improved the creep life by a factor of three in the baseline condition, because the precipitation of a third phase which caused localized interruptions in the lamellar structure was eliminated. The creep lives of single crystals with this lower Mo composition were increased by an additional factor of two, when the γ' size was refined prior to creep testing by an oil quench from the homogenization temperature. Thus, the directionally coarsened structure and the resulting creep properties can be altered significantly in a

specific alloy by changes in the initial microstructure produced prior to testing. It is hoped that this study may assist in the understanding and optimization of this unique microstructure in advanced single crystal turbine blade alloys.

References

(1) C. P. Sullivan, G. A. Webster, and B. J. Piearcey: J. Inst. Metals, vol. 96, 1968, pp. 274-281.

(2) R. G. Davies and T. L. Johnston: Proc. of 3rd Bolton Landing Conf. on Ordered Alloys, B. H. Kear et al., eds., p. 447, Claitors Publishing Division, Baton Rouge, LA, 1970.

(3) R. A. Stevens and P. E. J. Flewitt: Mat. Sci. Eng., vol. 37, 1979, pp. 237-247.

(4) D. D. Pearson, F. D. Lemkey, and B. H. Kear: Proc. 4th Int. Symp. on Superalloys, Seven Springs, PA, J. K. Tien et al., eds., p. 513, ASM, Metals Park, OH, 1980.

(5) D. D. Pearson, B. H. Kear and F. D. Lemkey: Creep and Fracture of Engineering Materials and Structures, p. 213, B. Wilshire and D. R. J. Owen, eds., Pineridge Press Ltd., Swansea, U. K., 1981.

(6) R. A. MacKay: Ph. D. Thesis, Case Western Reserve University, Cleveland, OH, to be published in 1984.

(7) C. Carry and J. L. Strudel: Acta Met., vol. 26, 1978, pp. 859-870.

(8) M. V. Nathal and L. J. Ebert: Scripta Met., vol. 17, 1983, pp. 1151-1154.

(9) G. A. Webster and B. J. Piearcey: Trans. ASM, vol. 59, 1966, pp. 847-859.

(10) A. Pineau: Acta Met., vol. 24, 1976, pp. 559-564.